Letter

Quantum diffusion induced by small quantum chaos

Hiroaki S. Yamada
Yamada Physics Research Laboratory, Aoyama 5-7-14-205, Niigata 950-2002, Japan

Kensuke S. Ikeda
College of Science and Engineering, Ritsumeikan University, Noji-higashi 1-1-1, Kusatsu 525-8577, Japan

(Received 25 August 2023; revised 18 March 2024; accepted 16 May 2024; published 3 June 2024)

It is demonstrated that quantum systems classically exhibiting strong and homogeneous chaos in a bounded region of the phase space can induce a global quantum diffusion. As an ideal model system, a small quantum chaos with finite Hilbert space dimension N weakly coupled with M additional degrees of freedom which is approximated by linear systems is proposed. By twinning the system the diffusion process in the additional modes can be numerically investigated without taking the unbounded diffusion space into account explicitly. Even though N is not very large, diffusion occurs in the additional modes as the coupling strength increases if $M \geqslant 3$. If N is large enough, a definite quantum transition to diffusion takes place through a critical subdiffusion characterized by an anomalous diffusion exponent.

DOI: 10.1103/PhysRevE.109.L062201

Introduction. By introducing any perturbation to completely integrable systems, a chaotic region is formed close to the nonlinear resonance which exists almost everywhere in the phase space. However, chaotic components are prevented to globalize by the KAM tori and are localized [1,2]. However, if such a small localized chaos interacts with some additional degrees of freedom, it can drive them and can change their energies on a large scale.

A typical example is the mechanism proposed by Arnold [3]. He showed that the entanglement between the stable and unstable manifolds of the unstable fixed point of a resonance, which causes the so called stochastic layer chaos, simultaneously leads to the intersection of stable and unstable manifolds with different energies of the additional degrees of freedom, thereby forming a global path to change their energy. Such kind of global instability is called the Arnold diffusion and were treated analytically and numerically [2,4–7]. The global motion induced by a localized small chaos such as the stochastic layer is an initiation leading to the intrinsically global ergodic motions [2,8–10].

Investigations of quantum Arnold diffusion for various systems elucidated that quantum motion mimics the classical delocalization [11–14]. However, the diffusion rate is much smaller than the classical one and very long-time behavior of the quantum diffusion is not known. It is expected to be suppressed by the quantum localization effect [13–15].

So far the quantum chaotic diffusion has been investigated extensively for "large" quantum chaos systems defined in unbounded phase space with infinite Hilbert-space dimension [16–19]. In such systems chaotic degrees of freedom itself may actively exhibit diffusion in the classical limit, but the diffusion is inhibited in its quantum counterparts due to the quantum localization effect. Such quantum localization is, however, destroyed, and classical diffusion is recovered [20,21] through Anderson-like transition if the number of degrees of freedom increases [18,19,22–25]. On the other hand, the nature of quantum diffusion passively induced by small quantum chaos system have not been known, although it is a fundamental problem closely related to the quantum global instability such as the Arnold diffusion.

In the present paper, we propose a simple model and method, with which we can examine whether or not a small quantum chaos can induce global diffusive motion along the modes contacting with it, and show that a global transportation is realized under appropriate conditions. "Small chaos" means chaotic systems confined to a finite region of the phase space by geometrical or dynamical conditions in the classical limit. As a first step, we examine small but sufficiently unstable chaos. Small and weakly unstable chaos such as stochastic layer will be investigated in forthcoming papers.

Model. As the first class of example, we consider strong and uniform chaotic systems called a C system or K system, bounded finitely by periodic boundaries [1], which are coupled with several numbers of unbounded additional degrees of freedom. The former is referred to as the main system and latter as the additional modes, respectively. The additional modes are supposed to be integrable if isolated, as is the example considered by Arnold. They are coupled weakly with the former at a small coupling strength characterized by the parameter η.

We suppose the integrable additional modes of number M is initially located at the action eigenstate $|I_{0k}\rangle$ $(1 \leqslant k \leqslant M)$ where $I_{0k} = \hbar \times$ integer. We approximate the Hamiltonian of the additional modes by linearizing around $I_k \sim I_{0k}$, and reset $\hat{I}_k - I_{0k}$ by $\hat{J}_k$. The Hamiltonian of the entire system is represented by

$$\hat{H}(\hat{p}, \hat{q}, \hat{J}, \hat{\phi}, t) = \hat{\mathcal{H}}(\hat{p}, \hat{q}, \hat{\phi}, t) + \hat{h}(\hat{\boldsymbol{J}})$$
$$\hat{\mathcal{H}}(\hat{p}, \hat{q}, \hat{\phi}, t) = \hat{p}^2/2 + V(\hat{q})\Delta(t) + \eta v(\hat{q}) w(\hat{\boldsymbol{\phi}})\Delta(t), \quad (1)$$

where $\Delta(t) := \sum_{n\in\mathbb{Z}} \delta(t-n)$ is the periodic delta-functional kicks. $\hat{h}(\hat{\boldsymbol{J}}) = \boldsymbol{\omega}\hat{\boldsymbol{J}}$, where $\hat{\boldsymbol{J}} = (\hat{J}_1, .., \hat{J}_M)$ and $\boldsymbol{\omega} = (\omega_1, ..., \omega_M)$ are the the linear frequencies at $I_k = I_{0k}(k = 1, ..., M)$. They are supposed to be mutually incommensurate. $\hat{\boldsymbol{\phi}} = (\hat{\phi}_1, ..., \hat{\phi}_M)$ are the angle operators conjugate to action operators $\hat{J}_k$ as $\hat{J}_k = -i\hbar\partial/\partial\phi_k$ in the c-number representation of $\hat{\phi}_k\,(0 \leqslant \phi_k \leqslant 2\pi)$. We take $w(\hat{\boldsymbol{\phi}}) := \sum_{k=1}^{M} w(\hat{\phi}_k)$, where $w(\phi_k)$ is a 2π periodic function of angle variable ϕ_k with mean value zero.

Here, we take the main system represented by a kicked rotor driven by the periodic kick $\Delta(t)$ of period one applied to the potential $V(\hat{q})$, where $\hat{q} = \sum_q q|q\rangle\langle q|$ and $\hat{p} = \sum_p p|p\rangle\langle p|$ are the position and momentum operators with eigenvalues q and p, respectively.

The main system is confined in the bounded phase space $-\pi \leqslant p \leqslant \pi$, $-\pi \leqslant q \leqslant \pi$, and the periodic boundary conditions are imposed on p and q. Then they are quantized as $q = \ell\hbar$ and $p = \ell'\hbar$, where ℓ, ℓ' are the integers satisfying $-N/2 \leqslant \ell, \ell' \leqslant N/2$ with N being the Hilbert-space dimension of the main system related to the Planck constant as $\hbar = 2\pi/N$.

Next, we take the Arnold cat map $V(\hat{q}) = K\hat{q}^2/2$ or the standard map $V(\hat{q}) = K\cos\hat{q}$ defined in the above bounded phase space as the main system $H_0(\hat{p}, \hat{q}, t)$. Taking $K(\in \mathbb{Z})$ as $K > 4$ or $K < 0$ (cat map) or $|K| \gg 1$(standard map), the main system can be made a C system and approximately a K system, respectively, which are (almost) uniformly chaotic with a flat invariant measure in the classical limit. The interaction terms $v(q)$ and $w(\phi)$ are period 2π functions of q and ϕ, respectively, with zero mean for the uniform invariant measure. We choose $v(q) = \cos(q)$ and $w(\phi_k) = \cos\phi_k$ of the interaction term in this paper. The similar model with linear oscillators have been used by several authors while studying the chaotic dynamics of the rotors [26] and Anderson transition of the atomic matter waves [27,28].

A great merit of using the linear oscillators as the additional mode is that the unitary evolution operator $\hat{U}(t) = \mathcal{T}\exp\{-i\int_0^t \hat{H}(\hat{p}, \hat{q}, \hat{J}, \hat{\phi}, s)ds/\hbar\}$ can be factorized into the action-dependent part and angle-dependent part as

$$\hat{U}(t) = e^{-i\hat{h}(\hat{\boldsymbol{J}})t/\hbar}\hat{\mathcal{U}}(t, \hat{\boldsymbol{\phi}}),$$
$$\hat{\mathcal{U}}(t, \hat{\boldsymbol{\phi}}) := \mathcal{T}e^{-\frac{i}{\hbar}\int_0^t \hat{\mathcal{H}}(\hat{p},\hat{q},\hat{\boldsymbol{\phi}}+\boldsymbol{\omega}s)ds}, \tag{2}$$

where $\mathcal{T}$ means the time-ordering operator. If the operator $\hat{X}$ does not contain the angle operators, the time evolved operator $\hat{X}(t) = \hat{U}^\dagger\hat{X}\hat{U}$ is dominated by $\hat{\mathcal{U}}(t)$ as $\hat{X}(t) = \hat{\mathcal{U}}(t)\hat{X}\hat{\mathcal{U}}(t)$. The action $\hat{J}(t)$ changes only at the $t = n(n \in \mathbb{Z})$-th kick. The Heisenberg equation of motion $d\hat{J}/dt = i[\hat{\mathcal{H}}, \hat{J}]/\hbar$ is integrated at each kick to lead to

$$\hat{J}_k(t) - \hat{J}_k(0) = -\sum_{n=1}^{[t]} \eta v(\hat{q}(n))w'(\hat{\phi}_k + \omega_k n), \tag{3}$$

where [ ] is the Gauss symbol and $w'(\phi_k) := dw(\phi_k)/d\phi_k$. Our interest is whether or not the chaotic motion of the main system can induce a global transport in the action space starting from $|\boldsymbol{J} = 0\rangle$. The physical quantity directly measuring the transported distance is the mean square displacement (MSD) of the action: $\Delta J_k(t)^2 := \langle\Psi_0|(\hat{J}_k(t) - \hat{J}_k(0))^2|\Psi_0\rangle$ $(k = 1, 2..., M)$, where $|\Psi_0\rangle = |\psi_0\rangle|\boldsymbol{J} = 0\rangle$ and $|\psi_0\rangle$ is the initial state of the main system. Classically, Eq. (3) describes a typical situation in which chaos induces diffusion in the additional modes: if the main system is fully chaotic, the "force" $v(q(n))w'(\phi_k + \omega_k n)$ is completely random with zero mean, and the classical variable $\Delta J_k(t)$ exhibits a Brownian motion. To compute the MSD or higher-order moment, we need not explicitly take the infinite Hilbert dimension of the J space into account as shown below.

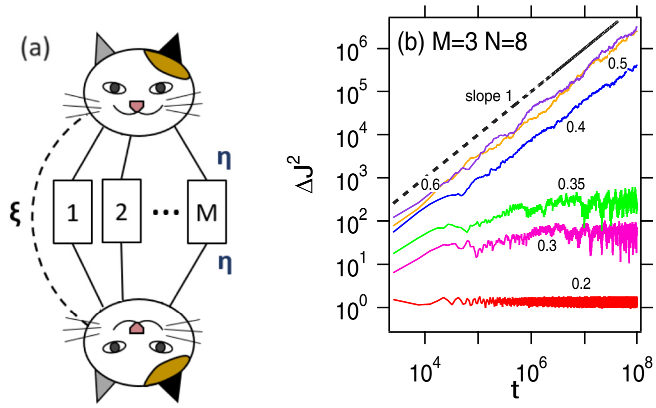

FIG. 1. (a) An Illustration of the twinned system with the coupling strength η and ξ. (b) The double-logarithmic plots of $\Delta J^2(t)$ as a function of time for the cat map of $K = -1$ and $N = 8$ coupled with three linear modes ($M = 3$). The result for various η in the range $\eta \in [0.2, 0.6]$ is shown.

Method. We twin the two identical parts represented by the Hamiltonian $\hat{\mathcal{H}}(\hat{p}, \hat{q}, \hat{\boldsymbol{\phi}}, t)$ of Eq. (1) and its paired one $\hat{\mathcal{H}}(\hat{p}', \hat{q}', \hat{\boldsymbol{\phi}}, t)$. Returning t to the continuous time representation, the Hamiltonian $\hat{H}_T$ of the twinned system is

$$\hat{H}_\xi^T = \hat{\mathcal{H}}_\xi^T(\hat{p}, \hat{q}, \hat{\boldsymbol{\phi}}, t) + h(\hat{\boldsymbol{J}})$$
$$\hat{\mathcal{H}}_\xi^T := \hat{\mathcal{H}}(\hat{p}, \hat{q}, \hat{\boldsymbol{\phi}}, t) + \hat{\mathcal{H}}(\hat{p}', \hat{q}', \hat{\boldsymbol{\phi}}, t) + \xi\hat{W}(\hat{\phi}_k, t). \tag{4}$$

The second part is spanned by the coordinate basis $|q\rangle'$ or the momentum basis $|p\rangle'$, and $\hat{q}' := \sum_q q|q\rangle'\langle q|'$ and $\hat{p}' := \sum_p p|p\rangle'\langle p|'$ are its coordinate and momentum operators, respectively. $\hat{W}$ is the interaction between the twinned parts given by

$$\hat{W}(\hat{\phi}_k, t) := w'(\hat{\phi}_k)\sum_q v(q)(|q\rangle\langle q|' + |q\rangle'\langle q|)\Delta(t-0), \tag{5}$$

The twin system is illustrated in Fig. 1(a). The interaction between the twins takes place just at $t = n + 0 (n \in \mathbb{Z})$ after the periodic kick. We define here the transition operators $\hat{R}^+ = \sum_q |q\rangle'\langle q|$ and $\hat{R}^- = (\hat{R}^+)^\dagger$. Since our system is formed by twins and the noninteracting Hamiltonian $\hat{H}_{\xi=0}^T$ commutes with $\hat{R}^\pm$, the time-evolved operators $\hat{R}^\pm$ change only in the moments of the interaction at $t = n + 0$. Let $\hat{U}_\xi^T(t)$ and $\hat{\mathcal{U}}_\xi^T(t)$ be the time evolution operator of the Hamiltonian $\hat{H}_\xi^T$ and $\hat{\mathcal{H}}_\xi^T(\hat{p}, \hat{q}, \hat{\boldsymbol{\phi}} + \boldsymbol{\omega}t)$, respectively. Then the relation similar to Eq. (2) holds and $\hat{R}^\pm(t)$ is dominated by $\hat{\mathcal{H}}_\xi^T(\hat{p}, \hat{q}, \hat{\boldsymbol{\phi}} + \boldsymbol{\omega}t)$.

As a result, we obtain

$$(\hat{R}^{+}(t)-\hat{R}^{+}(0))/\xi = \frac{i}{\hbar}\sum_{s=1}^{[t]}[v(\hat{q}(s))-v(\hat{q}'(s))]w'(\hat{\phi}_k+\omega_k s). \tag{6}$$

We suppose initially the second chaotic system is not populated, and only the first main system and the additional modes are started from the same initial condition as the original system given by Eq. (1). Here the coupling strength ξ of the twinned system is chosen at the smallest level that the numerical precision allows. The RHS of Eq. (6) is computed in the lowest order with respect to ξ. Then the second term of RHS, which contains only the population operator of the second system, can be neglected, and the LHS of Eq. (6) is identified with $\hat{J}_k(t)-\hat{J}_k(0)$. The MSD is thus related to the excitation number $\hat{R}^{+}\hat{R}^{-}$ as

$$\begin{aligned}\Delta J_k(t)^2 &:= \langle\Psi_0|(\hat{J}_k(t)-\hat{J}_k(0))^2|\Psi_0\rangle \\ &= \langle\Psi_0|(\hat{R}^{+}(t+0)-\hat{R}^{+}(0))(\hat{R}^{-}(t+0) \\ &\quad -\hat{R}^{-}(0))|\Psi_0\rangle/\xi^2 \\ &\simeq \frac{\hbar^2\eta^2}{(2\pi)^M\xi^2}\int d\boldsymbol{\phi}\sum_q\left|\langle q|'\hat{\mathcal{U}}_\xi^T(t,\boldsymbol{\phi})|\psi_0\rangle\right|^2, \end{aligned}\tag{7}$$

where $\int d\boldsymbol{\phi}=\int_0^{2\pi}\ldots\int_0^{2\pi}\Pi_k^M d\phi_k$. As mentioned above, $\hat{\mathcal{U}}_\xi^T(t,\boldsymbol{\phi})=\mathcal{T}\exp\{-i\int_0^t\hat{\mathcal{H}}_\xi^T(\hat{p},\hat{q},\boldsymbol{\phi}+\boldsymbol{\omega}s,s)ds/\hbar\}$, which can be expressed as the product of a step-by-step evolution operator. More detailed derivations and remarks about Eqs. (6) and (7) can be found in the Supplemental Material [29]. In the following we omit k from $\hat{J}_k$ and J_k if not necessary. Intuitively, the twins are designed such that their interaction mimics the force causing the diffusion of J [the RHS of Eq. (3)], and the MSD of J is copied to the total excitation number of the second system of the twins.

The higher-order moment can also be evaluated in the same way. The integration over the phase variables $\boldsymbol{\phi}$ means to take quantum mechanical average with respect to the initial action state $|\boldsymbol{J}=\boldsymbol{0}\rangle=\int_0^{2\pi}\ldots\int_0^{2\pi}d\boldsymbol{\phi}|\boldsymbol{\phi}\rangle/(2\pi)^{M/2}$ which is very efficiently carried out by replacing the integral by the average over quasirandom numbers of the integer(ν)-multiplied irrational number $\phi_k=\nu\chi_k(0\leqslant\nu\leqslant\nu_{\max})$, where χ_k are irrational numbers.

We have only to execute the numerical wavepacket evolution with $\hat{\mathcal{U}}_\xi^T(t,\boldsymbol{\phi})$ using $2N$-dimensional basis for a fixed c-number $\phi_k=\nu\chi_k$ starting from $|\psi_0\rangle$, and compute the integrand of Eq. (7) for a fixed $\phi_k=\nu\chi_k$, and next take the average over the $\nu_{\max}$ data. Finally the average over the results for randomly chosen initial state $|\psi_0\rangle$ is taken.

We compared the result of the twinning method with the result of the direct wavepacket propagation in the full Hilbert space spanned by the truncated set of action basis and the N-dimensional basis of the main system. The results agree well, which are demonstrated in the Supplemental Material [29].

Result. We first take the chaotic cat map as the main system, which induces the ideal diffusion process according to Eq. (3) in the classical model. However, the quantum version follows the classical chaotic diffusion at least in a certain period of time evolution. Indeed, in the case of $M=1$, the diffusion is suppressed and the MSD reaches to an upper bound $\xi_L^2:=\Delta J^2(t=\infty)$ (for brevity the index k is omitted). We call ξ_L the quantum localization length. As seen in Fig. 2(a), numerically $\xi_L\propto N^2D_{cl}$, where D_{cl} is a classical diffusion constant proportional to η^2 for the hyperbolic cat map, [immediately derived from Eq. (3) with the delta-correlated classical force]. For $M=2$, the classical diffusion is still suppressed, but the numerical observation tells that localization length is enhanced and increases exponentially as $\xi_L\propto\exp\{D_{cl}N^2\}=\exp\{c_1\eta^2N^2\}$, where c_1 is a numerical constant [see Fig. 2(b)]. Similar phenomena have been observed in large quantum chaos systems with infinite Hilbert dimension, such as perturbed standard map [30] and perturbed Anderson map [31].

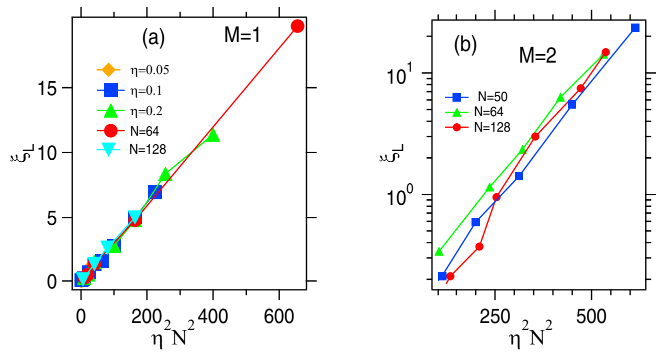

FIG. 2. The dynamical localization length of the linear mode J_1 obtained for some different system parameters is plotted as a function of $\eta^2N^2(\propto\eta^2D_{cl})$. (a) $M=1$ and (b) $M=2$. Note that the vertical axis is in the linear scale for $M=1$ and in the logarithmic scale for $M=2$, respectively.

As $M\geqslant 3$, things change drastically: for small enough η the MSD still saturates at a finite level and the quantum localization still remains, but as η is taken large enough the MSD increases linearly without limit at least for t less than 10^8. Figure 1(b) shows that such a drastic change is observed even for very small main systems with N of only eight. The border between the localization and the normal diffusion is not, however, very definite at all. On the other hand, as N increases greater than 10^2, the transition from localization to the normal diffusion becomes very definite. Figure 3 presents a typical example of $N=256$. There exists a critical value $\eta=\eta_c$ below which the MSD saturates and above which the MSD increases to reach to the normal diffusion. And just at $\eta=\eta_c$ the MSD increases according to an anomalous diffusion law $\Delta J^2(t)\propto t^\alpha$ with a characteristic exponent α $(0\leqslant\alpha\leqslant1)$. Figure 3(b) shows the temporal behavior of MSD around $\eta=\eta_c$ by using the time-dependent characteristic exponent $\alpha(t)$ defined by

$$\alpha(t)=\frac{d\log\overline{\Delta J^2(t)}}{d\log(t)}, \tag{8}$$

where the over bar $\overline{X(t)}$ means to take a local time average of $X(t)$. Equation (8) implies $\overline{\Delta J^2(t)}$ increases $t^{\alpha(t)}$ locally at t.

Figure 3(b) shows the $(t,\alpha(t))$ plot for various η. Below η_c, $\alpha(t)$ decreases monotonically to zero, while it increases to reach the normal diffusion $\alpha=1$ above η_c, which provides a strong evidence that a definite transition from the

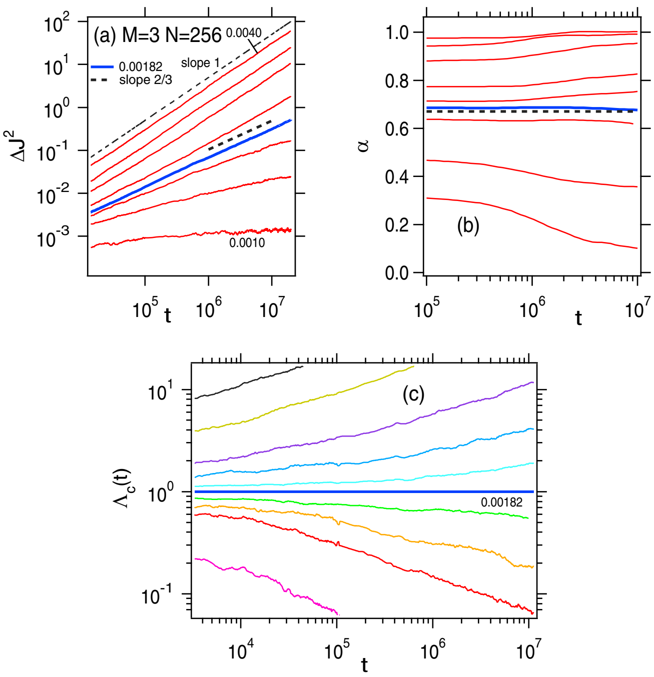

FIG. 3. (a) The double-logarithmic plots of $\Delta J^2(t)$ as a function of time for the cat map ($K = -1$, $N = 256$) with three linear modes ($M = 3$). The results for $\eta_c \simeq 0.00182$ is shown in a thick blue line. The broken lines with the slope 1 and 2/3 are shown. (b) The instantaneous diffusion index $\alpha(t)$ for some ϵ. The broken line indicates the critical subdiffusion line $\alpha(t) = \alpha_c = 2/3$ predicted by the scaling theory. (c) The scaled MSD $\Lambda_c(t)$ as functions of time for the increasing interaction strength η.

localization to the normal diffusion without limit takes place. Just at $\eta = \eta_c$, $\alpha(t)$ takes a constant value α_c and MSD exhibits an anomalous diffusion $\Delta J^2_{\eta=\eta_c}(t) \propto t^{\alpha_c}$. As η exceeds η_c, the diffusion constant approaches to the classical diffusion constant $D_{cl} \propto \eta^2$.

Once η_c is decided by the $(t, \alpha(t))$ plot, the critical behavior close to η_c can be more directly captured by the scaled representation of MSD $\Lambda_c(t) := \Delta J^2(t)/\Delta J^2_{\eta=\eta_c}(t)$ as shown in Fig. 3(c). The critical value η_c decreases very rapidly with N, which will be discussed later.

The localization-diffusion transition is always observed if $M \geqslant 3$ and the MSD increases according to the subdiffusion $\Delta J^2(t) \propto t^{\alpha_c}$ at the critical η_c, which decreases as $\eta_c \sim N^{-3/2}$, as shown in Fig. 4(a), if $N \gg 1$. According to the numerical observation α_c is independent of N and depends only on M and decreases to zero with M. The critical value η_c also decreases with M as shown in Fig. 4(b). The results are summarized as

$$\alpha_c = \frac{2}{M}, \quad \eta_c \propto N^{-3/2}(M-2)^{-1}. \tag{9}$$

The diffusion phenomena can never be observed for the elliptic cat ($-4 < K < 1$), if $N \gg 1$ and η is small enough. The results mentioned above do not change if the main system is replaced by the standard map of $|K| \gg 1$ defined on a periodically bounded phase space.

The transition scheme through the critical subdiffusion $\Delta J^2(t) \sim t^{2/M}$ is very similar to the Anderson-like transition

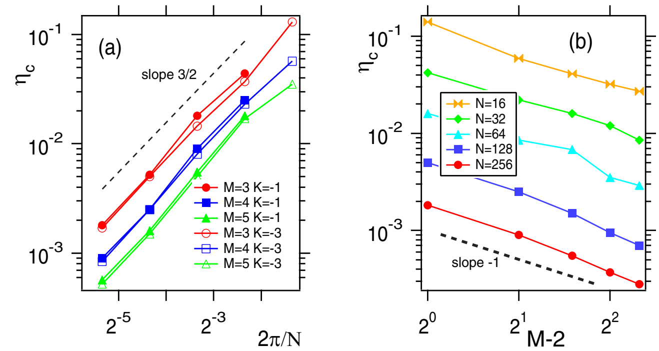

FIG. 4. (a) The critical perturbation strength η_c as a function of $\hbar = 2\pi/N$ for the cat map with $M = 3, 4, 5$ linear modes and $K = -1, -3$. The black broken line with a slope 3/2 is shown. (b) η_c as a function of $M - 2$ for $K = -1$. The black dotted line with a slope -1 is shown. Note that the data are plotted in double-logarithmic scale.

observed for standard map perturbed by multiple-periodic perturbations [22–24]. Although not shown here, the $\eta_c \propto N^{-3/2}$ can be derived by a conventional theory of Anderson transition. It is, however, basically different from ours in that the diffusive motion is supported by the chaotic degree of freedom itself. It is a large quantum chaotic system defined in an

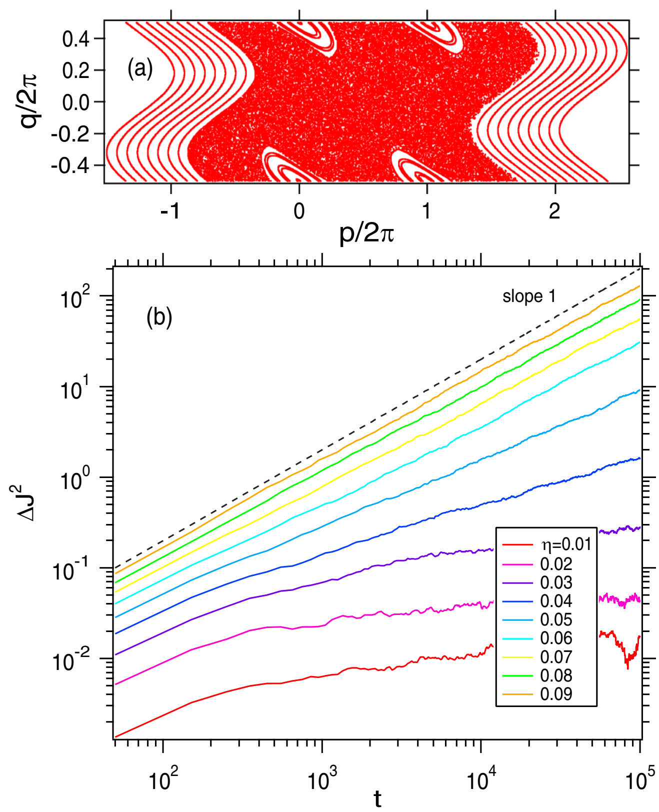

FIG. 5. (a) The classical Poincare map of the modified standard map, which manifests overlapped chaos around two resonances at $p = 0$ and $p = 2\pi$ is finitely bounded by tori. Here $K = 3.0$ and $M = 3$, and $p_{1,2} = \pi \pm 2\pi$. (b) Double logarithmic plots of MSD vs t for (a) are shown. Diffusion in the additional modes is recovered with increase in η, where $N = 256(\hbar = 2\pi/N)$.

infinitely extended phase space and is supported by infinite dimensional Hilbert space. Moreover, in our case, the transition to diffusion is quite different from the conventional Anderson transition for small N, which will be reported elsewhere.

An alternative model. Next, we examine a more natural case where a nonideal chaos generated by the overlap of two nonlinear resonances is bounded finitely not by the periodic boundaries but by regular orbits. We take a modified standard map defined as follows. The potential is $V(\hat{q}) = K\cos\hat{q}$ as usual, and the momentum space is unbounded. However, the kinetic energy takes the ordinary form $T(\hat{p}) = \hat{p}^2/2$ only in a bounded region $I := [p_1, p_2]$, and $T(\hat{p})$ is replaced by linear functions $a\hat{p} + b$ out of I. The constants a and b are decided such that $T(\hat{p})$ is continuous and smooth at p_1 and p_2. It is easy to show the classical motion outside of I is completely integrable. By choosing p_1 and p_2 adequately, we can confine the two resonances at $p = 0$ and $p = 2\pi$, which yields chaotic motion by the overlap of resonances for $K > 1$, as is illustrated in Fig. 5(a). Thus our system models a typical situation of a small classical chaos bounded by regular regions.

We examined the above system by our method. The obtained result is not so simple as the ideal case of the cat map, but we confirmed that the normal diffusion is recovered for $M \geqslant 3$ following a similar scenario as the cat map. We show in Fig. 5(b) the transition process of MSD together with the classical Poincare plot of the main system.

Conclusion. In conclusion we investigated whether small quantum chaos can induce quantum diffusion leading to the global transportation. As a simplest model we proposed a small but strong quantum chaos system coupled very weakly with additional linear modes. The existence of diffusion depends seriously on the number M, and for $M \geqslant 3$ global diffusion is induced even for small Hilbert space dimension N. If $N \gg 1$, the diffusion is realized through a critical state exhibiting an anomalous diffusion as the coupling strength exceeds a weak quantum critical value. In the present work we examined sufficiently unstable chaotic systems in the classical limit as the main system. More interesting is the case of small and weakly unstable chaos typically exemplified by the stochastic layer. In the latter case the global transportation process along the linear modes corresponds to a quantum Arnold diffusion, and its existence is a quite interesting problem.

Acknowledgments. This work is supported by Japanese people's tax via MEXT/JSPS KAKENHI Grants No. 22K03476 and No. 22H01146, and the authors would like to acknowledge them. The authors are also thankful to Kankikai (Dr. T. Tsuji) and Koike memorial house for using the facilities during this study.

[1] A. J. Lichtenberg and M. A. Lieberman, *Regular and Chaotic Dynamics*, Applied Mathematical Sciences Vol. 38 (Springer, New York, NY, 1992).
[2] B. V. Chirikov, Phys. Rep. **52**, 263 (1979).
[3] V. I. Arnol'd, Soviet Mathematics-Doklady **5**, 581 (1964).
[4] N. N. Nekhoroshev, Russ. Math. Surv. **32**, 1 (1977).
[5] M. A. Lieberman, Ann. N.Y. Acad. Sci. **357**, 119 (1980).
[6] P. J. Holmes and J. E. Marsden, J. Math. Phys. **23**, 669 (1982).
[7] K. Kaneko and Richard J. Bagley, Phys. Lett. A **110**, 435 (1985).
[8] P. M. Cincotta, C. Efthymiopoulos, C. M. Giordano, and M. F. Mestre, Physica D **266**, 49 (2014).
[9] M. S. Santhanam, S. Paul, and J. BharathiKannan, Phys. Rep. **956**, 1 (2022).
[10] S. S. Maurya, J. B. Kannan, K. Patel, P. Dutta, K. Biswas, J. Mangaonkar, M. S. Santhanam, and U. D. Rapol, Phys. Rev. E **106**, 034207 (2022).
[11] Y. Boretz, and L. E. Reichl, Phys. Rev. E **93**, 032214 (2016).
[12] D. M. Leitner and P. G. Wolynes, Phys. Rev. Lett. **79**, 55 (1997).
[13] V. Y. Demikhovskii, F. M. Izrailev, and A. I. Malyshev, Phys. Rev. Lett. **88**, 154101 (2002).
[14] V. Y. Demikhovskii, F. M. Izrailev, and A. I. Malyshev, Phys. Rev. E **66**, 036211 (2002).
[15] V. Y. Demikhovskii, F. M. Izrailev, and A. I. Malyshev, Phys. Lett. A **352**, 491 (2006).
[16] G. Casati, B. V. Chirikov, F. M. Izraelev, and J. Ford, in *Stochastic Behavior in Classical and Quantum Hamiltonian Systems*, edited by G. Casati and J. Ford (Springer-Verlag, Berlin, 1979), pp 334.
[17] S. Fishman, D. R. Grempel, and R. E. Prange, Phys. Rev. Lett. **49**, 509 (1982).
[18] G. Casati, I. Guarneri, and D. L. Shepelyansky, Phys. Rev. Lett. **62**, 345 (1989).
[19] L. Chotorlishvili, S. Stagraczynski, M. Schlerc, and J. Berakdar, Acta Phys. Pol. A **135**, 1155 (2019).
[20] S. Adachi, M. Toda, and K. Ikeda, Phys. Rev. Lett. **61**, 659 (1988).
[21] B. Gadway, J. Reeves, L. Krinner, and D. Schneble, Phys. Rev. Lett. **110**, 190401 (2013).
[22] M. Lopez, J. F. Clement, P. Szriftgiser, J. C. Garreau, and D. Delande, Phys. Rev. Lett. **108**, 095701 (2012).
[23] M. Lopez, J.-F. Clement, G. Lemarie, D. Delande, P. Szriftgiser, and J. C. Garreau, New J. Phys. **15**, 065013 (2013).
[24] H. S. Yamada and K. S. Ikeda, Phys. Rev. E **101**, 032210 (2020).
[25] See for Anderson transition, e.g., B. Kramer and A. MacKinnon, Rep. Prog. Phys. **56**, 1469 (1993); P. Markos, Acta Phys. Slov. **56**, 561 (2006); *50 Years of Anderson Localization*, edited by E. Abrahams (World Scientific Singapore, 2010).
[26] D. L. Shepelyansky, Physica D **8**, 208 (1983).
[27] J. Chabe, G. Lemarie, B. Gremaud, and D. Delande, P. Szrifigiser, and J. C. Garreau, Phys. Rev. Lett. **101**, 255702 (2008).
[28] G. Lemarié, J. Chabé, P. Szriftgiser, J. C. Garreau, B. Grémaud, and D. Delande, Phys. Rev. A **80**, 043626 (2009).
[29] See Supplemental Material at http://link.aps.org/supplemental/10.1103/PhysRevE.109.L062201 for details on the derivation and the numerical test of the twinning method.
[30] I. Manai, J. F. Clement, R. Chicireanu, C. Hainaut, J. C. Garreau, P. Szriftgiser, and D. Delande, Phys. Rev. Lett. **115**, 240603 (2015).
[31] H. S. Yamada, F. Matsui, and K. S. Ikeda, Phys. Rev. E **97**, 012210 (2018).